

OSIRIS

Optical, Spectroscopic, and Infrared Remote Imaging
System

Rosetta-Osiris

To

Planetary Science Archive Interface Control Document

RO-RIS-MPAE-ID-015

Issue: 3

Revision: f

20 Oct 2015

Prepared by:

Pablo Gutierrez-Marques



Document Change Record

Iss./Rev.	Date	Pages affected	Description
Draft/-	4 Nov. 2003	All	First draft
1a	29 Aug 2005	All	Fleshed out
1b	24 Jan 2006	All	Added science objectives General cleaning
2a	2 Nov 2006	All	Major cleaning and reorganization of document Added dataset overview covering the period until Comet encounter Changed the PDS file naming convention to be PDS compliant Simplified the data directory structure Moved most of the actual PDS label information to the EDR/SIS document.
3a	14/5-2009	All	Added data set ID's separated between NAC and WAC
3c	2/12-2010	All	Synchronized the EAICD with the actual archive generation process (several minor points) Added description of new EXTRAS directory used to store the BROWSE HTML files, thumbnail images and activity log
3d	28/1-2011		Added missing BROWSE directory description Corrected mistakes in the data set ID description Corrected various spelling errors
3e	3/3-2011	26	Change CAL description to reflect the non zip based implementation required by the PDS
3f	20 Oct 2015	1,2,9,26	Added explanation on the extent of the calibration database Updated PI and creator of the data

1 Table Of Contents

1	TABLE OF CONTENTS	3
2	INTRODUCTION	5
2.1	PURPOSE AND SCOPE	5
2.2	ARCHIVING AUTHORITIES	5
2.3	CONTENTS	6
2.4	INTENDED READERSHIP	6
2.5	APPLICABLE DOCUMENTS	6
2.6	ACRONYMS AND ABBREVIATIONS	7
2.7	CONTACT NAMES AND ADDRESSES	9
2.8	SCIENTIFIC OBJECTIVES	10
2.9	THE COMETARY NUCLEUS	10
2.9.1	<i>Position and size of the nucleus</i>	10
2.9.2	<i>Rotational state</i>	10
2.9.3	<i>Shape, volume, and density</i>	10
2.9.4	<i>Nucleus formation and surface topography</i>	11
2.9.5	<i>Colour, mineralogy, and inhomogeneity</i>	11
2.9.6	<i>Surface photometry</i>	12
2.9.7	<i>Polarization measurements</i>	12
2.9.8	<i>Active and inactive regions</i>	12
2.9.9	<i>Physics of the sublimation process</i>	12
2.9.10	<i>The diurnal cycle</i>	13
2.9.11	<i>Outbursts</i>	13
2.9.12	<i>Mass loss rate</i>	13
2.9.13	<i>Characterisation of the landing site</i>	13
2.9.14	<i>Observation of the Philae touchdown</i>	13
2.10	NEAR-NUCLEUS DUST	14
2.10.1	<i>Detection of emission at rendezvous</i>	14
2.10.2	<i>Temporal evolution</i>	14
2.10.3	<i>Large particles in bound orbits</i>	15
2.10.4	<i>How inactive are 'inactive' regions?</i>	15
2.10.5	<i>Optical properties of the dust</i>	15
2.10.6	<i>Eclipses</i>	15
2.10.7	<i>Acceleration and fragmentation</i>	16
2.11	GAS EMISSIONS	16
2.11.1	<i>Selected species</i>	16
2.11.2	<i>Sublimation process and inactive areas</i>	16
2.12	SERENDIPITOUS OBSERVATIONS	17
2.12.1	<i>Asteroid fly-bys</i>	17
2.12.2	<i>Mars fly-by</i>	17
2.12.3	<i>Earth-Moon system fly-bys</i>	17
3	OVERVIEW OF INSTRUMENT DESIGN, DATA HANDLING PROCESS AND PRODUCT GENERATION	18
3.1	INSTRUMENT DESIGN	18
3.1.1	<i>The Narrow Angle Camera</i>	18
3.1.2	<i>The wide angle camera (WAC)</i>	19
3.2	DATA HANDLING PROCESS	20
3.3	DATA SET AND DATA PRODUCT OVERVIEW	21
3.4	OVERVIEW OF DATA PRODUCTS	25
3.4.1	<i>Instrument Calibrations</i>	25
3.5	DATA SET ORGANIZATION	26
3.5.1	<i>The DATA directory</i>	26



3.5.2	<i>The CALIB directory</i>	26
3.5.3	<i>The SOFTWARE directory</i>	29
3.5.4	<i>The CATALOG directory</i>	30
3.5.5	<i>The DOCUMENT directory</i>	30
3.5.6	<i>The INDEX directory</i>	30
3.5.7	<i>The BROWSE directory</i>	31
3.5.8	<i>The EXTRAS directory</i>	31
3.6	DATA FILE NAMING CONVENTIONS AND PRODUCT IDS	32
3.6.1	<i>Filenaming Convention</i>	32
3.6.2	<i>The Dataset ID</i>	33
3.7	STANDARDS USED IN DATA PRODUCT GENERATION	35
3.7.1	<i>PDS Standards</i>	35
3.7.2	<i>Time Standards</i>	35
3.7.3	<i>Reference Systems</i>	36
4	PDS OBJECT AND KEYWORD DEFINITIONS	38

2 Introduction

2.1 Purpose and Scope

The purpose of this EAICD (Experimenter to (Science) Archive Interface Control Document) is two fold. First it provides users of the Osiris instrument with detailed description of the product and a description of how it was generated, including data sources and destinations. Secondly, it is the official interface between the OSIRIS instrument team and the PSA archiving authority.

2.2 Archiving Authorities

The Planetary Data System Standard is used as archiving standard by

- NASA for U.S. planetary missions, implemented by PDS
- ESA for European planetary missions, implemented by the Research and Scientific Support Department (RSSD) of ESA

ESA implements an online science archive, the PSA, to support and ease data ingestion to offer additional services to the scientific user community and science operations teams as e.g. search queries that allow searches across instruments, missions and scientific disciplines several data delivery options as direct download of data products, linked files and data sets ftp download of data products, linked files and data sets

The PSA aims for online ingestion of logical archive volumes and will offer the creation of physical archive volumes on request.

2.3 Contents

This document describes the data flow of the Osiris instrument on the Rosetta mission from the s/c until the insertion into the PSA for ESA. It includes information on how data were processed, formatted, labeled and uniquely identified. The document discusses general naming schemes for data volumes, data sets, data and label files. Standards used to generate the product are explained. Software that may be used to access the product is explained further on.

The design of the data set structure and the data product is given. Examples of these are given in the appendix.

2.4 Intended Readership

The staff of the archiving authority (Planetary Science Archive, ESA, RSSD, design team) and any potential user of the Osiris data.

2.5 Applicable Documents

Planetary Data System Preparation Workbook, February 1, 1995, Version 3.1, JPL, D-7669, Part1

Planetary Data System Standards Reference, June 1, 1999, Version 3.3, JPL, D-7669, Part 2

[Mission] Archive Generation, Validation and Transfer Plan, [month day, year], [doc number]

OSIRIS EDR/SIS (RO-RIS-MPAE-ID-018)

2.6 Acronyms and Abbreviations

ASCII	American Standard Code for Information Interchange
ADC	Analog Digital Converter
CRB	CCD Readout Board
CCD	Charge Coupled Device
DDS	Data Distribution System
DPU	Data Processing Unit
DSP	Digital Signal Processor
EDR	Experiment Data Record
ESA	European Space Agency
HK	House Keeping data
IAA	Instituto de Astrofísica de Andalucía
IDA	Institut fuer Datentechnik und Kommunikationsnetze
INTA	Instituto Nacional de Técnica Aeroespacial
JPEG	Joint Photographic Experts Group (Common compressed image format)
LAM	Laboratoire d'Astrophysique de Marseille
MCB	Motor Controller Board
MLI	Multi Layer Insulation
MPS	Max Planck Institut für Sonnensystemforschung
NAC	Narrow Angle Camera
OSIRIS System	Optical, Spectroscopic, and Infrared Remote Imaging
PCM	Power Converter Module
PDS	Planetary Data Systems
RDR	Reduced Data Record
RSSD	Research and Scientific Support Department (ESA)
RO	Rosetta Orbiter
OIOR	Orbiter Instrument Operational Request
ODL	Object Description Language
PSA	Planetary Science Archive
SPICE	Spacecraft, Planet, Instrument, C-matrix, Event kernels
SIS	Software Interface Specification
SPIHT	Set Partitioning in Hierarchical Trees (Wavelet compression algorithm)
TBC	To Be Considered
TBD	To Be Determined



TMI	TeleMetry Image
UPD	University of Pardia
UPM	Universidad Politécnica de Madrid
WAC	Wide Angle Camera

2.7 Contact Names and Addresses

Holger Sierks

Max Planck Institut für Sonnensystemforschung

Justus-von-Liebig Weg 3

D-37077 Göttingen

Germany

Phone: (+49) 551 384 979 242

email: sierks@mps.mpg.de

Pablo Gutierrez-Marques

Max Planck Institut für Sonnensystemforschung

Justus-von-Liebig Weg 3

D-37077 Göttingen

Germany

Phone: (+49) 551 384 979 313

email: gutierrez@mps.mpg.de

2.8 Scientific objectives

2.9 The cometary nucleus

The imaging systems on the Giotto and Vega spacecraft were remarkably successful in providing our first glimpses of a cometary nucleus and its immediate environment. Reviews of the results of these investigations can be found, *e.g.* in Keller *et al.* (1996). Despite this success, the imaging results were limited and many questions were left unanswered, and additional questions arose, many of which will be addressed by OSIRIS. We describe here the goals of our nucleus observations.

2.9.1 Position and size of the nucleus

The first goal of OSIRIS will be to localise the cometary nucleus and to estimate its size and shape as quickly as possible for mission planning purposes. These properties must be coarsely known well before the mapping phase commences. This should be performed near the end of the approach phase when the spacecraft is between 103 and 104 km from the nucleus. Determination of the radius to an accuracy of 10 % from 10⁴ km can be performed with the NAC and will immediately yield an estimate of the nucleus volume (and mass for an assumed density) accurate to about a factor of 2.

2.9.2 Rotational state

The goal of OSIRIS is to determine the rotational properties of the comet including the periods of rotation about three principal axes, the total angular momentum vector L , the changing total spin vector and the characteristics of any precessional behaviour. Measurements of these quantities will constrain the inhomogeneity of the nucleus and will also permit the development of time-dependent templates over which other data sets may be laid. The secondary, more ambitious goal is to use OSIRIS to monitor the rotational properties throughout the entire mission to search for secular evolution in response to the torques acting on the nucleus caused by the onset of jet activity as the comet approaches perihelion. Model calculations indicate that for a small nucleus, such as 67P/Churyumov-Gerasimenko, torques could force re-analysis of the rotational properties of the nucleus on timescales of days (Gutiérrez *et al.*, 2005). The measured precession rate, along with an estimate of the average reaction force (from the non-gravitational acceleration of the nucleus) and an estimate of the torque caused by outgassing, may allow an estimate of the absolute value of the nucleus moment of inertia. This, in turn, would give clues to the internal density distribution, especially when combined with the gravity field determination (see Pätzold *et al.*, this volume), allowing us to distinguish between a lumpy, a smoothly varying, and a homogeneous nucleus (see also Kofman *et al.*, this volume). The structural inhomogeneity would provide an important clue for the size distribution of the forming planetesimals.

2.9.3 Shape, volume, and density

The concept of comets as uniformly shrinking spherical ice balls was shattered by the Giotto results. The nucleus is expected to be highly irregular on all scales as a consequence of cratering, outgassing, and non-uniform sublimation (Keller *et al.*, 1988). However, it is not clear whether these irregular-shaped bodies reflect the shape of the nuclei at their formation, or are the result of splitting during their evolution, or are caused by non-uniform sublimation.

To accurately model such a craggy shape, techniques developed at Cornell University (Simonelli *et al.*, 1993) can be used. Although OSIRIS has no stereo capability *per se*, the motion of Rosetta relative to the nucleus can be used to produce stereo pairs. The shape model will be based upon these

stereogrammetric measurements in addition to limb and terminator observations. Once the shape model is available, it can be used to determine the surface gravity field and moments of inertia and will also be used to reproject and mosaic digital images, as well as to develop surface maps. This technique has yielded accurate shapes for the Martian moons and Galileo's asteroid targets, 951 Gaspra and 243 Ida (Thomas *et al.*, 1995; 1994).

To look for internal inhomogeneities of say 30 % implies that differences in the geometrical and dynamical moments of inertia need to be known to better than 10 %. We therefore need to measure both to better than 1 %. Thus, the topography must be characterised over the entire nucleus to an accuracy of ± 20 m.

2.9.4 Nucleus formation and surface topography

On the smallest scales, the building blocks comprising the cometary nucleus may be a heterogeneous mixture of interstellar and interplanetary dusts and ices, with a structure and composition reflecting the physical conditions and chemistry of the protoplanetary disc. The different accretion processes leading to the production of first, grains, then, building blocks and, finally, cometary nuclei, are all expected to have left their mark on a nucleus which has remained largely unaltered since its formation. OSIRIS will therefore perform a detailed investigation of the entire cometary surface over a range of spatial scales as wide as possible to identify the hierarchy of cometary building blocks.

In addition to its implications for nucleus formation, the topography of the surface determines the heat flow in the uppermost layers of the nucleus (Gutierrez *et al.*, 2000, Colwell *et al.*, 1997). High resolution imaging will determine the normal to the surface and hence provide input to surface heat flow calculations.

The Vega 2 TVS observations of jets were interpreted as showing a fan generated from a few, kilometre-long, quasi-linear cracks (Smith *et al.*, 1986; Sagdeev *et al.*, 1987). If fresh cracks appear on the surface during the aphelion passage, then OSIRIS will be able to probe the inner layers of the nucleus where some stratification is expected from the loss of volatiles near the surface.

2.9.5 Colour, mineralogy, and inhomogeneity

Inhomogeneity of mineral composition and colour could provide the most obvious clues to the size of building blocks. The Vega and Giotto cameras were able to determine only rough estimates of the broad-band ($\lambda/\Delta\lambda = 5$) colour of the nucleus of 1P/Halley. OSIRIS will allow a much more sophisticated study of the mineralogy of the nucleus surface by recording images that span the entire wavelength range from 250 nm - 1000 nm.

OSIRIS also has the opportunity to search for specific absorption bands associated with possible mineral constituents. The wavelengths of pyroxene absorptions are highly dependent upon their exact structure (Adams, 1974). Hence, filters giving complete coverage of the 750 nm to 1 μ m regions at 60 nm resolution were incorporated. Vilas (1994) suggested that the 3.0 μ m water of hydration absorption feature of many low albedo (including C-class) asteroids strongly correlates with the 700 nm $\text{Fe}^{2+} \rightarrow \text{Fe}^{3+}$ oxidised iron absorption feature. Given the spectral similarity between C-class asteroids and 1P/Halley and the high water ice content in comets, a search for the water of hydration feature at 700 nm will be made.

2.9.6 Surface photometry

Due to the limited information from high-velocity fly-bys, little was learned of the photometric properties of the surface of comet 1P/Halley. The correct determination of the phase function for comet 67P/Churyumov-Gerasimenko will provide information on the surface roughness through application of, for example, Hapke's scattering laws. The Philae observations will provide the parameters necessary to validate the surface roughness models used to interpret global data provided by OSIRIS.

2.9.7 Polarization measurements

The properties which can be addressed by polarization measurements can be obtained more accurately by observations of the surface from the Philae or by *in situ* analysis. Implementation of polarization measurements in OSIRIS was thought costly in terms of resources and calibration and they were therefore not included.

2.9.8 Active and inactive regions

Modelling (Kührt and Keller, 1994) suggests that debris from active regions will not choke the gas and dust production in view of the highly variable terrain, the extremely low gravity, and the lack of bonding between particles forming the debris. Inactive regions can only arise if either the material comprising the regions formed in the absence of volatiles or, alternatively, if the regions have become depleted in volatiles without disrupting the surface.

To verify this picture, a comparison of active and inactive regions on comet 67P/Churyumov-Gerasimenko must be of high priority. If inactive regions are merely volatile-depleted with respect to active regions, high signal-to-noise observations at several wavelengths may be required to differentiate between the two. Imaging of the interface between active and inactive regions may provide evidence of surface structures and tensile strength present in one type of region, but not in the other.

As the observations of 'filaments' indicate (Thomas and Keller, 1987), there is no reason to suppose that active regions are homogeneous. Activity may be restricted within an active region (see for example the theoretical calculations of Keller *et al.*, 1994). For this reason, OSIRIS will identify the active fraction within what we call an active region. Achieving this goal may lead to understanding how cometary activity ceases, leaving an inert comet. Do inactive spots within active regions spread to reduce cometary activity or does the infall of material from the edge of the sublimation crater choke emission?

Directions of jets and locations of active spots are influenced by topography. The distribution and orientation of near-nucleus jets can be used to infer topographic features (Thomas *et al.*, 1988, Huebner *et al.*, 1988). OSIRIS will investigate these correlations.

2.9.9 Physics of the sublimation process

The physical processes characterising the sublimation and erosion processes in or above active regions depend on the physical structure of the surface and the distribution of refractory and volatile material within the nucleus. Dust particles have usually been treated as impurities in the ice (icy conglomerate).

Starting with the interpretation of the images of 1P/Halley (Keller, 1989), it has become clear that the topography requires a matrix dominated by refractory material (Küppers *et al.*, 2005). The other extreme is the model of a friable sponge, where the refractory material is intimately mixed with the ice and where the erosion process maintains a balance between the ice and dust. How are dust particles lifted off the surface? The excellent resolution of the OSIRIS NAC, which will be smaller than the mean free path of the gas near the surface, will allow the detection and study of the relevant macrophysical processes.

2.9.10 The diurnal cycle

OSIRIS will be able to monitor short-term changes in active regions very easily. Changes are most likely when active regions cross the terminators. Cooling will lead to decreased activity, but on what timescale? On the other hand, as the insolation increases, will there be changes in the surface structure?

2.9.11 Outbursts

Outbursts (or rapid increases in the brightness of cometary comae) have frequently been observed from the ground and recently also during the approach of the Deep Impact spacecraft to comet 9P/Tempel 1. This implies some sudden increase or even explosion of activity ripping the surface crust apart. OSIRIS, and in particular the WAC, can be used to monitor autonomously the nucleus activity over many months at various scales. The NAC can then be used to look in detail at the source to determine how the site has altered topographically and spectrally.

2.9.12 Mass loss rate

The floor of the active regions will be lower by several metres on average after the passage of comet 67P/Churyumov-Gerasimenko through its perihelion. It is clear that if an active area can be monitored by OSIRIS at a resolution of ≈ 30 cm the mass loss will be evident. If the density of the surface layer can be determined by Philae or through joint OSIRIS/Radio Science investigations, this is potentially the most accurate means to determine the total mass loss rate particularly if the mass loss is dominated by infrequently emitted large particles.

2.9.13 Characterisation of the landing site

The NAC was designed to remain in focus down to 1 km above the nucleus surface. Mapping at ~ 2 cm px⁻¹ will reveal inhomogeneities of the nucleus at scale lengths comparable to the size of Philae. Homogeneous sites would provide no difficulties in interpretation but heterogeneous sites may be scientifically more interesting. As a result, OSIRIS needs to be able to characterise the landing site and to identify on what types of terrain Philae has landed.

2.9.14 Observation of the Philae touchdown

There is no guarantee that the orbiter will be able to observe Philae when it strikes the surface. However, OSIRIS will provide valuable information on the impact velocity, the result of the initial impact, and the final resting position and orientation.

Outgassing from the impacted site may also occur. If fresh ice is so close to the surface that the lander can penetrate the crust, emission of gas and dust may be fairly vigorous. If so, OSIRIS can quantify this emission with highest possible spatial and temporal resolution.

2.10 Near-nucleus dust

The near-nucleus dust environment of a comet is remarkably complex and remains poorly understood. Understanding the near-nucleus environment is necessary to understanding the nucleus itself. OSIRIS can investigate global dust dynamics.

2.10.1 Detection of emission at rendezvous

OSIRIS will be used to place constraints on distant activity of the nucleus. It is evident, however, that detection of dust in the vicinity of the nucleus will be extremely difficult at high heliocentric distances. The dust production may decrease as steeply as $r_h^{-2.9}$ (Schleicher *et al.*, 1998), with a corresponding decrease in flux proportional to $r_h^{-4.9}$. At 3.25 AU, we estimate the ratio of the signal received from the dust to that from the surface (I_d/I_s) $\approx 4 \cdot 10^{-4}$ based on scaling of Giotto measurements. Therefore, to quantify the total dust production rate, a dynamic range of > 2000 is required. Both the WAC and the NAC were designed with this contrast requirement.

2.10.2 Temporal evolution

2.10.2.1 Variation with heliocentric distance

HMC observations showed that the dust production rate of comet 1P/Halley during the Giotto fly-by was remarkably stable over the three hours of the encounter. Ground-based observations have shown, however, that comets exhibit large and rapid changes in dust production. A key goal of OSIRIS will be therefore to monitor the variation in the production rate and to compare it to the rotational characteristics of the nucleus and the change in r_h .

2.10.2.2 Variations with rotation

The lack of significant variation in the dust production rate with the rotation seen at comet 1P/Halley was not expected. How does the production vary with the solar zenith angle? How long does an active region take to switch on after sunrise? These phenomena are determined by the physical properties (*e.g.* the thermal conductivity) of the surface layer. If sublimation occurs below the surface then a period of warming may be required before dust emission starts. The surface layer could act as a buffer to stabilise the activity. These questions can be addressed using OSIRIS to monitor the active region during the first minutes after it comes into sunlight.

2.10.2.3 Night side activity and thermal inertia

The inferred absence of night side activity during the Giotto fly-by and the thermal map created from near-infrared spectral scans of comet 9P/Tempel 1 during the recent Deep Impact mission (A'Hearn *et al.*, 2005) suggest that the thermal inertia must be low. Observations of comet Hale-Bopp (C/1995 O1) also suggest that the thermal inertia of comets is low (Kührt, 2002). The high porosity of the surface and the resulting low thermal conductivity suggest that the activity should decrease rapidly and stop when the energy source is removed. Monitoring the dust emission as an active region crosses the evening terminator can confirm this hypothesis.

2.10.2.4 Short-term variability

The dust emission from the nucleus of comet 1P/Halley showed no evidence for short-term (order of minutes) temporal variations. Because of the nature of the active regions one might expect, however, that the emission should occasionally show an enhanced or reduced rate on a timescale of perhaps a few seconds. A sudden burst offers the possibility of following the emitted dust and using it to derive streamlines and velocities in the flow. This would provide strong constraints on the hydrodynamics of the flow and lead to increased understanding of the dust-gas interaction a few metres above active regions. If large enough, outbursts could also modify the flow field itself allowing us to use OSIRIS to monitor the reaction of the inner coma to changes in the emission rate.

2.10.3 Large particles in bound orbits

It was shown that gravitationally-bound orbits around cometary nuclei are possible, in theory, for relatively small particles even in the presence of radiation pressure (Richter and Keller, 1995). In addition, evidence from radar measurements suggests that large clouds of centimetre-sized objects accompany comets in their orbits (Campbell *et al.*, 1989). The high resolving power of OSIRIS combined with our proximity to the nucleus will allow us to place constraints on the number density of objects with a particle radius of $a > 5$ mm. Since it is now widely believed that most of the mass lost by comets is in the form of large particles (McDonnell *et al.*, 1991), observations of this phenomenon could prove very important in determining the dust to gas ratio. Clearly, it would be a major discovery to find an extremely large chunk which might be termed ‘a satellite’ of the nucleus. Active chunks, as seen in comet Hyakutake (Rodionov *et al.*, 1998), may also be evident.

2.10.4 How inactive are ‘inactive’ regions?

The observations by HMC and more recent fly-bys (A’Hearn *et al.*, 2005) were not good enough to place firm constraints on the activity of so-called inactive regions. Dust emission from the illuminated but apparently inactive regions could have been up to 10% of the emission from active regions and remained undetected. This clearly has implications for the evolution of the nucleus and for the flow field of gas and dust emission about the nucleus.

2.10.5 Optical properties of the dust

The orbit of Rosetta and the broad-band filters in OSIRIS will allow observations of dust at many phase angles (0° - 135°) over a wide wavelength range. The phase curve and colour are sensitive to particle size, composition, and roughness. Deduction of these properties and their variation with r_h will be important for ground-based observations of other comets since it will provide the single scattering albedo, the phase function, and the characteristic particle size.

2.10.6 Eclipses

Eclipse measurements are extremely interesting for the innermost dust coma as they would allow OSIRIS to determine the forward scattering peak of the dust phase function, which provides the best information on the size distribution, and nature of the dust particles. The strong forward scattering peak also yields the most sensitive measurement of the dust column density (*e.g.* Divine *et al.*, 1986).

2.10.7 Acceleration and fragmentation

Complications with the determination of local dust production rates arise if the observations cover the dust acceleration region, if fragmentation is significant, or if optical depth effects become important. Measurements of the acceleration will quantify the drag coefficient of the gas-particle interaction and characterise the near-surface Knudsen layer. The fluffiness of the cometary dust can be derived from these observations.

A complementary approach is to measure the radius and velocity of large escaping dust agglomerates in dependence of heliocentric distance. By knowing the gravitational forces, this would also provide information on the physics of the gas-dust interaction (drag coefficient) at and near the surface (Knudsen layer), on the cohesive forces, and on the density of the agglomerates.

2.11 Gas emissions

Our current understanding of the composition of the nucleus and variations within the nucleus is severely limited by our lack of knowledge about the processes in the innermost coma. We know little about the variations of the composition of the outgassing on any scale, although there are indications from Earth-based measurements of large-scale heterogeneity (*e.g.* in 2P/Encke and in 1P/Halley). There are distributed sources in the coma which produce some of the species in the coma, including H₂CO, CO, and CN. Because we cannot separate completely the extended coma source from the nuclear source, we cannot determine reliably the amount of ice in the nucleus. We therefore plan to make observations of the gas in order to address some of the most crucial questions in relating abundances in the coma to abundances in the nucleus.

2.11.1 Selected species

In order to constrain the heterogeneity of other parent molecules, we will map the release of certain daughter species in the vicinity of the nucleus. Dissociation products having short lifetimes and identifiable parents are ideal for this task. In particular, NH at 336.5 nm and NH₂ at 570 nm will be measured to trace the heterogeneity of NH₃ (and thus the nitrogen chemistry in the nucleus), CS at 257 nm to trace the heterogeneity of CS₂ (and thus the sulphur chemistry), and OH at 309 nm and OI at 630 nm to trace H₂O.

The heterogeneity of other fragments, such as CN (388 nm), will also be measured, even though we do not know the identity of the parent molecules, because these species show evidence of an extended source. The recent interest in the distribution of Na has led us to introduce a sodium filter at 589 nm.

2.11.2 Sublimation process and inactive areas

The results from 1P/Halley showed us that the release of dust is confined to discrete active areas, comprising only a small fraction of the surface (15 %). We have no information, however, on whether the gas is similarly confined. One of the key questions to be answered is whether gas is also released from the apparently inactive areas. The mapping capability of OSIRIS is ideally suited to answer this question and thereby to assess the effects of an inert layer on the release of gas and dust.

2.12 Serendipitous observations

2.12.1 Asteroid fly-bys

The fly-bys of 2867 Steins and 21 Lutetia will provide interesting secondary targets on the way to the comet. The main scientific goals of OSIRIS observations of the asteroids are:

- Determination of physical parameters (size, volume, shape, pole orientation, rotation period)
- Determination of surface morphology (crater abundance, crater size distribution, presence of features such as ridges, grooves, faults, boulders, search for the presence of regolith)
- Determination of mineralogical composition (heterogeneity of the surface, identification of local chemical zones, superficial texture)
- Search for possible gravitationally bound companions (detection of binary systems).

2.12.2 Mars fly-by

High-resolution images of Mars (> 200 px across the planet) can be taken within two days of closest approach (*cf.* recent HST images). This will provide data on the global meteorological conditions on Mars and allow us to follow weather patterns over a period of about two days. Images around 12 hours before closest approach would be of sufficient resolution to allow us to resolve vertical structures in the atmosphere at the limb and to estimate the global atmospheric dust content. The solar occultation during Mars fly-by would allow detection of the putative Martian dust rings.

2.12.3 Earth-Moon system fly-bys

As with the space missions Galileo and Cassini/Huygens, the Rosetta remote sensing instruments can perform testing and calibration during the fly-bys of the Earth-Moon system. There are also several interesting possibilities for new science. For example, the Moon is now known to have a tenuous sodium atmosphere ('exosphere'). The Na filter on the WAC can be used to acquire maps of Na near the Moon. Similarly, OI emission from the Earth may be detectable at high altitudes. Vertical profiles of OI in the atmosphere of the Earth can be derived by stellar occultations.

3 Overview of Instrument Design, Data Handling Process and Product Generation

3.1 Instrument Design

The OSIRIS camera system is composed of two telescopes; a. A Wide Angle Camera (WAC) and b. A Narrow Angle Camera (NAC)

3.1.1 The Narrow Angle Camera

The NAC uses an off axis three mirror optical design. The off axis design was selected in order to minimize the straylight reaching the CCD (The NAC has a proven stray light attenuation of better than $1.0e-9$). The optical beam is reflected of the three mirrors (M1, M2 and M3) before passing through a double filter wheel, a mechanical shutter mechanism and an anti radiation plate (ARP) before reaching the CCD. The detectors are back illuminated back thinned 2048x2048 pixel CCD's.



Figure 1 (right) The OSIRIS NAC flight unit in the lab. (left) The NAC Optical path

Optical design	3-mirror off-axis
Angular resolution	$18.6 \mu\text{rad px}^{-1}$
Focal length	717.4 mm
Mass	13.2 kg
Field of view	$2.20 \times 2.22^\circ$
F-number	8
Spatial scale from 100 km	1.86 m px^{-1}
Typical filter bandpass	40 nm
Wavelength range	250nm - 1000nm
Number of filters	12
Estimated detection threshold	18 mV

Table 1 Basic NAC parameters

3.1.2 The wide angle camera (WAC)

The WAC uses an off axis two mirror optical design. The off axis design was selected in order to minimize the stray light reaching the CCD (The NAC has a proven stray light attenuation of better than $1.0e-8$).

The optical beam is reflected of the two mirrors (M1 & M2) before passing through a double filter wheel, a mechanical shutter mechanism, an anti radiation plate (ARP) before reaching the CCD.



Figure 2 (left) The OSIRIS WAC flight unit in the lab. (right) The WAC Optical path

Optical design	2-mirror off-axis
Angular resolution	101 μ rad px-1
Focal length	140(sag)/131(tan)
Mass	9.48 kg
Field of view	11.34 x 12.11°
F-number	5.6
Spatial scale from 100 km	10.1 m px-1
Typical filter bandpass	5 nm
Wavelength range	240nm - 720nm
Number of filters	14
Estimated detection threshold	13 mV

Table 2 Basic WAC parameters

For more details please see the OSIRIS EDR/SIS included in the dataset documentation and the OSIRIS Space Science Review paper also included in the dataset documentation.

3.2 Data Handling Process

The OSIRIS EDR processing begins with the reconstruction of packetized telemetry data resident on the ESA DDS system by the IDA GSEOS (Ground Support Operating System) software system. The GSEOS system saves the image data as OSIRIS level 0 image files (TMI or PDS format depending on flight software version).

The OSIRIS level 0 images are then processed by a software application called tmi2pds used to calibrate the header information and to append various metadata like spacecraft position and orientation. The output is stored as CODMAC level 2 PDS compliant image files (EDR's).

The EDR's are then processed by an IDL coded image processing pipeline used to generate CODMAC level 3 files (RDR's). The CODMAC level 3 data contains radiometrically calibrated image data. The CODMAC level 3 data will then be passed through another pipeline that will remove the optical distortion of the cameras and output CODMAC level 4 data files.

The full data flow is illustrated in Figure 3 and the processing levels are defined in Table 3.

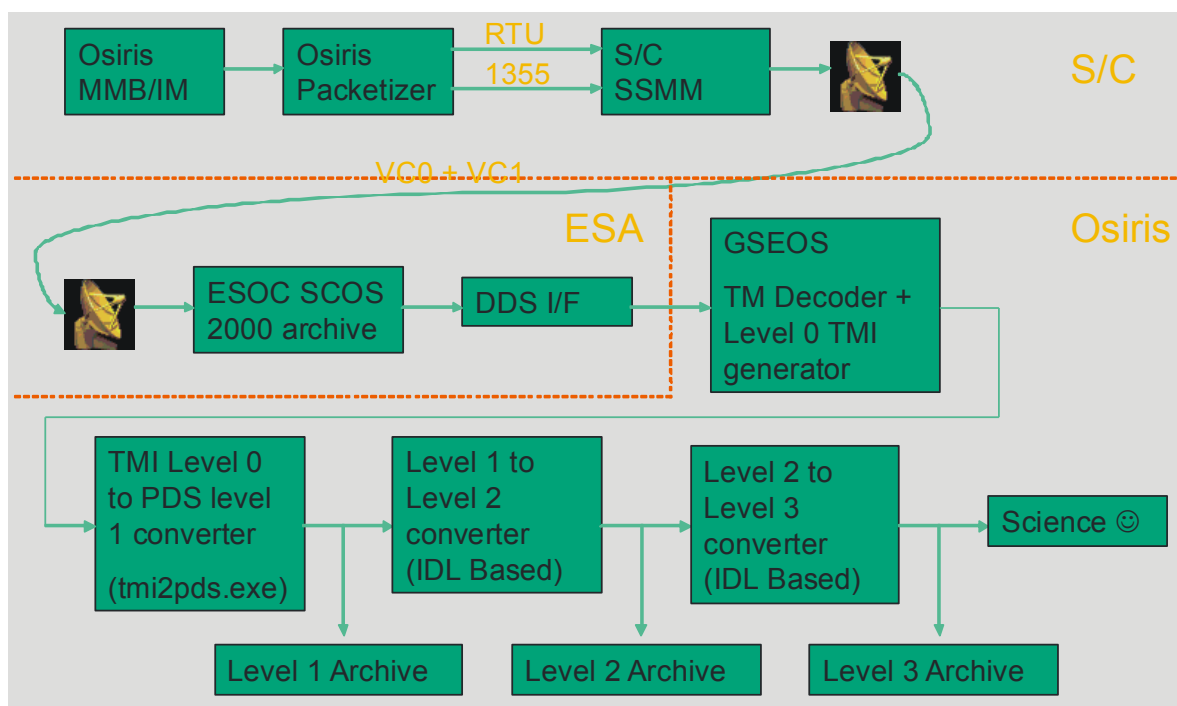


Figure 3 The OSIRIS data and processing flow

OSIRIS Data Levels	CODMAC levels	Description
Packet Data	1	Telemetry data stream as received at the ground station, with science and engineering data embedded.
0		PDS or TMI formatted data files. Uncalibrated header and uncalibrated image data
1	2	PDS compliant data files with calibrated header data and uncalibrated image data
2	3	PDS compliant data files with calibrated header data and calibrated image data
3	4	PDS compliant data files with calibrated header data and calibrated image data optical distortion removed
4	5	PDS compliant data files with calibrated header data and calibrated image data optical distortion removed and image rotated to align image y-axis with galactic north.

Table 3 OSIRIS and CODMAC data levels

3.3 Data Set and Data Product Overview

For the period until arrival at comet 67P/Churyumov-Gerasimenko OSIRIS will archive the following datasets in the PSA:

Dataset	CODMAC Level	Mission Phase	Expected time of delivery
RO-X-OSINAC-2-CVP-COMMISSIONING-V1.1	2	COMMISSIONING	Nov 2006
RO-X-OSIWAC-2-CVP-COMMISSIONING-V1.1	2	COMMISSIONING	Nov 2006
RO-X-OSINAC-3-CVP-COMMISSIONING-V1.1	3	COMMISSIONING	Nov 2006
RO-X-OSIWAC-3-CVP-COMMISSIONING-V1.1	3	COMMISSIONING	Nov 2006
RO-X-OSINAC-2-CR2-CRUISE_2-V1.0	2	CRUISE 2	Feb 2007
RO-X-OSIWAC-2-CR2-CRUISE_2-V1.0	2	CRUISE 2	Feb 2007
RO-X-OSINAC-3-CR2-CRUISE_2-V1.0	3	CRUISE 2	Feb 2007
RO-X-OSIWAC-3-CR2-CRUISE_2-V1.0	3	CRUISE 2	Feb 2007
RO-X-OSINAC-2-MARS-MARS_SWING-BY-V1.0	2	MARS SWING-BY	Jan 2008



RO-X-OSIWAC-2-MARS-MARS_SWING-BY-V1.0	2	MARS SWING-BY	Jan 2008
RO-X-OSINAC-3-MARS-MARS_SWING-BY-V1.0	3	MARS SWING-BY	Jan 2008
RO-X-OSIWAC-3-MARS-MARS_SWING-BY-V1.0	3	MARS SWING-BY	Jan 2008
RO-X-OSINAC-2-EAR2-EARTH_SWING-BY_2-V1.0	2	EARTH SWING-BY 2	Jul 2008
RO-X-OSIWAC-2-EAR2-EARTH_SWING-BY_2-V1.0	2	EARTH SWING-BY 2	Jul 2008
RO-X-OSINAC-3-EAR2-EARTH_SWING-BY_2-V1.0	3	EARTH SWING-BY 2	Jul 2008
RO-X-OSIWAC-3-EAR2-EARTH_SWING-BY_2-V1.0	3	EARTH SWING-BY 2	Jul 2008
RO-X-OSINAC-2-CR4A-CRUISE_4-1-V1.0	2	CRUISE 4-1	Jan 2009
RO-X-OSIWAC-2-CR4A-CRUISE_4-1-V1.0	2	CRUISE 4-1	Jan 2009
RO-X-OSINAC-3-CR4A-CRUISE_4-1-V1.0	3	CRUISE 4-1	Jan 2009
RO-X-OSIWAC-3-CR4A-CRUISE_4-1-V1.0	3	CRUISE 4-1	Jan 2009
RO-X-OSINAC-2-AST1-STEINS_FLY-BY-V1.0	2	STEINS FLY-BY	May 2009
RO-X-OSIWAC-2-AST1-STEINS_FLY-BY-V1.0	2	STEINS FLY-BY	May 2009
RO-X-OSINAC-3-AST1-STEINS_FLY-BY-V1.0	3	STEINS FLY-BY	May 2009
RO-X-OSIWAC-3-AST1-STEINS_FLY-BY-V1.0	3	STEINS FLY-BY	May 2009
RO-X-OSINAC-2-CR4B-CRUISE_4-2-V1.0	2	CRUISE 4-2	Apr 2010
RO-X-OSIWAC-2-CR4B-CRUISE_4-2-V1.0	2	CRUISE 4-2	Apr 2010
RO-X-OSINAC-3-CR4B-CRUISE_4-2-V1.0	3	CRUISE 4-2	Apr 2010
RO-X-OSIWAC-3-CR4B-CRUISE_4-2-V1.0	3	CRUISE 4-2	Apr 2010
RO-X-OSINAC-2-EAR3-EARTH_SWING-BY_3-V1.0	2	EARTH SWING-BY 3	Jun 2010
RO-X-OSIWAC-2-EAR3-EARTH_SWING-BY_3-V1.0	2	EARTH SWING-BY 3	Jun 2010
RO-X-OSINAC-3-EAR3-EARTH_SWING-BY_3-V1.0	3	EARTH SWING-BY 3	Jun 2010
RO-X-OSIWAC-3-EAR3-	3	EARTH SWING-BY 3	Jun 2010



EARTH_SWING-BY_3-V1.0			
RO-X-OSINAC-2-CR5-CRUISE_5-V1.0	2	CRUISE 5	Dec 2010
RO-X-OSIWAC-2-CR5-CRUISE_5-V1.0	2	CRUISE 5	Dec 2010
RO-X-OSINAC-3-CR5-CRUISE_5-V1.0	3	CRUISE 5	Dec 2010
RO-X-OSIWAC-3-CR5-CRUISE_5-V1.0	3	CRUISE 5	Dec 2010
RO-X-OSINAC-2-AST2-LUTETIA_FLY-BY-V1.0	2	LUTETIA FLY-BY	Apr 2011
RO-X-OSIWAC-2-AST2-LUTETIA_FLY-BY-V1.0	2	LUTETIA FLY-BY	Apr 2011
RO-X-OSINAC-3-AST2-LUTETIA_FLY-BY-V1.0	3	LUTETIA FLY-BY	Apr 2011
RO-X-OSIWAC-3-AST2-LUTETIA_FLY-BY-V1.0	3	LUTETIA FLY-BY	Apr 2011
RO-X-OSINAC-2-RVM1-RENDEZVOUS_MANOEUVRE_1-V1.0	2	RENDEZVOUS MANOEUVRE 1	Feb 2012
RO-X-OSIWAC-2-RVM1-RENDEZVOUS_MANOEUVRE_1-V1.0	2	RENDEZVOUS MANOEUVRE 1	Feb 2012
RO-X-OSINAC-3-RVM1-RENDEZVOUS_MANOEUVRE_1-V1.0	3	RENDEZVOUS MANOEUVRE 1	Feb 2012
RO-X-OSIWAC-3-RVM1-RENDEZVOUS_MANOEUVRE_1-V1.0	3	RENDEZVOUS MANOEUVRE 1	Feb 2012
RO-X-OSINAC-2-CR6-CRUISE_6-V1.0	2	CRUISE 6	Aug 2014
RO-X-OSIWAC-2-CR6-CRUISE_6-V1.0	2	CRUISE 6	Aug 2014
RO-X-OSINAC-3-CR6-CRUISE_6-V1.0	3	CRUISE 6	Aug 2014
RO-X-OSIWAC-3-CR6-CRUISE_6-V1.0	3	CRUISE 6	Aug 2014
RO-X-OSINAC-2-RVM2-RENDEZVOUS_MANOEUVRE_2-V1.0	2	RENDEZVOUS MANOEUVRE 2	Mar 2015
RO-X-OSIWAC-2-RVM2-RENDEZVOUS_MANOEUVRE_2-V1.0	2	RENDEZVOUS MANOEUVRE 2	Mar 2015
RO-X-OSINAC-3-RVM2-RENDEZVOUS_MANOEUVRE_2-V1.0	3	RENDEZVOUS MANOEUVRE 2	Mar 2015

RO-X-OSIWAC-3-RVM2- RENDEZVOUS_MANOEUVRE_2- V1.0	3	RENDEZVOUS MANOEUVRE 2	Mar 2015
--	---	---------------------------	----------

Table 4 Expected OSIRIS dataset covering the period until arrival at comet 67P/Churyumov-Gerasimenko

OSIRIS is not archiving any pre launch/ground calibration data because of file format incompatibility issues.

3.4 Overview of Data Products

For details on the OSIRIS EDR and RDR PDS labels please see the OSIRIS EDR/SIS document included in the dataset documentation folder.

3.4.1 Instrument Calibrations

OSIRIS is archiving calibrated data (CODMAC level 3). The software used to generate the calibrated data is included in the archived dataset structure. Please note that this software is included for information only.

The OSIRIS calibration software relies on three parts:

- CALIB/DATABASE.ZIP containing a database of calibration information
(please see readme.txt file in the root of the ZIP archive)
- SOFTWARE/FWPDSLIB.ZIP containing an IDL (Interactive Data Language) software library for manipulating PDS images.
- SOFTWARE/OSIRIS_CAL.ZIP containing the OSIRIS calibration pipeline itself (as an IDL software package)

The overall flow of the calibration pipeline is illustrated in Figure 4.

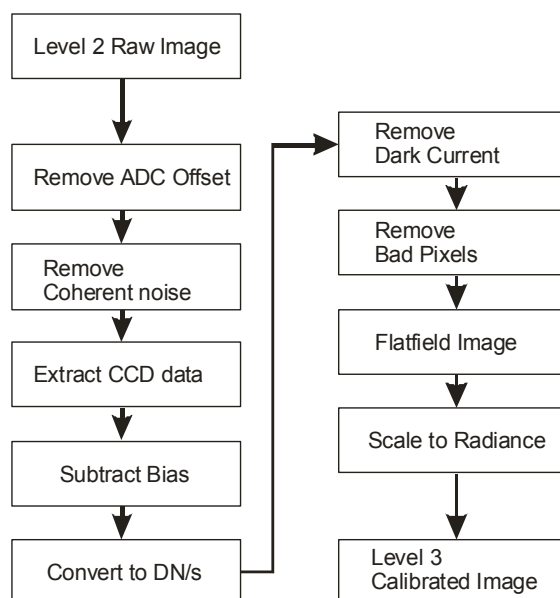


Figure 4 OSIRIS calibration pipeline overview

More details about the OSIRIS calibration flow can be found in the document OSIRIS_CAL.pdf included in the DOCUMENT folder of the datasets.

3.5 Data Set Organization

The OSIRIS flight data sets are organized using the subdirectories recommended by the PDS standards:

- DATA
- CALIB
- EXTRAS
- SOFTWARE
- CATALOG
- DOCUMENT
- INDEX
- BROWSE

3.5.1 The DATA directory

The data directory contains the actual OSIRIS EDR and RDR data files. The DATA directory contains a list of sub directories. Each of these subdirectories will contain all data acquired within a calendar month. The directories are named:

YYYY-MM

Example: 2006-12 will contain all data acquired in the month of December 2006

3.5.2 The CALIB directory

The CALIB directory provides various calibration parameters for OSIRIS. These parameters are used by the OSIRIS calibration pipeline IDL software package found in the SOFTWARE folder.

The CALIB folder contains the various database information required to calibrate OSIRIS images. The information provided is stored in a format readable by the OSIRIS calibration pipeline software (located in the SOFTWARE folder) which may not always follow the PDS standard. All information is, however, either readable using either a text editor (ascii format) of a std PDS data file reader (PDS image data and PDS table data).

Given that the calibration database is considered a single product even if it can be used separately to calibrate images from the NAC and the WAC, it is delivered in its entirety on the NAC and WAC datasets.

The calibration database has the following structure:

CALIB/		
	ABSCAL/	Folder containing the DN/s to W/m ² /sr/nm for various optical filter combinations
	ADC/	Folder containing the low/high adc offset valid for the various amplifier combinations
	BIAS/	Folder containing the bias offsets for the various operational

		modes of OSIRIS
	DISTORSION/	Folder containing the optical distortion model parameters for the cameras
	FILTERS/	Folder containing the filter transmission curves for the various optical filters
	FLATFIELDS/	Folder containing the flatfields for the various filter combinations
	MIRRORS/	Folder containing the mirror reflectivity curves (for both single mirror and for full optical path)
	QE	The CCD quantum efficiency
	SHUTTER	Folder containing calibration parameters for the two shutter mechanisms of the cameras
	SOLARFLUX	Folder constraining a solar reference spectrum

ABSCAL:

Contains files with the format <camera>_<model>_AbsCal_V<version>_<Creation Date>.txt

The data files contains <tag>=<value> lists with the format:

abs<filter>_A contains the absolute calibration constant for <filter> [(DN/s) / (W/m²/nm/sr)]

abs<filter>_A_Err contains an error estimate for abs<filter>_A

abs<filter>_T contains the average transmission coefficient for <filter>

ADC:

Contains the ADC offset added to the images by the readout electronics for various readout configuration

The data files contain <tag>=<value> lists with the format:

adc_offset_a contains the ADC offset for amplifier chain A

adc_offset_b contains the ADC offset for amplifier chain B

adc_offset_ab contains the ADC offset for amplifier chain AB

BIAS:

Contains the BIAS offset added to the images by the readout electronics for various readout configuration

The data files contains <tag>=<value> lists with the format:

<WIN Mode>_<Binning>_<amplifier>_SYNC<sync value>

FILTERS:

Contains filter transmission curves for the various optical filter that can be placed in the optical beam

The folder contains files with the names: <camera>_<model>_<filter name>_V<version>_<creation date>.tab

the first column contains the wavelength [nm]

the second column contains the transmission [fraction]

the third column contains the reflectivity of the filter surface

FLATFIELDS:

Contains the flatfield required to calibration OSIRIS images

The folder contains files with the names: <camera>_<model>_<filter number>_V<version>_<creation date>.img

The data files are stored in a data format that can be read with a PDS image reader

MIRRORS:

Contains the reflectivity curves for the mirrors of OSIRIS

The folder contains files with the names: <camera>_<model>_MIRROR_V<version>_<creation date>.tab

The data files are tabular text files where:

the first column contain the wavelength [nm]

the second column contain the single mirror reflectance

the third column contain the integrated mirror response of the full optical system

QE:

Contains the quantum efficiency of the OSIRIS CCD's

The folder contains files with the names:

<camera>_<model>_QE_V<version>_<creation date>.img (std calibration file)

or

<camera>_<model>_QE-<temperature>_V<version>_<creation date>.img
(temperature calibration file)

The data files are tabular text files with:

the first column giving the wavelength [nm]

the second column giving the QE of the CCD at wavelength

the third column giving the reflectivity of the CCD at wavelength

SHUTTER:

Contains parameters describing the transfer function from shutter pulse index to CCD physical location.

The folder contains files with the names: <camera>_<model>_SHM-B<blade>_V<version>_<creation date>.txt

The shutter motion transfer function is described as:

$$d(n) = d0 + L(\sin(th0) + \sin(n*\text{deg_per_stripe} + thZ - th0))$$

where n is the pulse index and d(n) is the distance moved by the shutter blade. The other parameters are found in the calibration file as <tag>=<value> data

3.5.3 The SOFTWARE directory

The SOFTWARE folder is used to store the software used to calibrate the OSIRIS images found in level 3 and higher.

Please note that the calibration software is included for information only. The actually calibrated data will be delivered separately as higher level datasets

The software folder contains two zip files:

- | | |
|-----------------|---|
| FWPDSLIB.ZIP: | A zip archive files containing an IDL (Interactive Data Language) library for manipulating PDS formatted data |
| OSIRIS_CAL.ZIP: | A zip archive containing the actual calibration software (IDL source files) |

Both zip files contains readme files describing installation and use at the root of the file

3.5.4 The CATALOG directory

The Catalog directory contains the catalog files required by the PDS standard:

DATASET.CAT	Description of the dataset
INSTHOST.CAT	Description of the the Rosetta orbiter spacecraft
MISSION.CAT	Description of the Rosetta mission
OSIRIS.CAT	Description of the OSIRIS instrument
PERSONNEL.CAT	Contact information
REFERENCE.CAT	References
TARGETS.CAT	Description of the target object observed in the dataset
SOFTWARE.CAT	Description of the included software packages

3.5.5 The DOCUMENT directory

The Document directory contains supporting documentation for the data set. The documents are organized in sub directories. Each subdirectory contains multiple versions of the same document. An ascii version of the document is always available (PDS requirement) but an ADOBE PDF version is typically also available.

Content:

[CALIB]	Short document describing the calibration process
[EAICD]	Archive interface control document (this Document)
[OSIRIS_SSR]	A Space Science Review paper describing the OSIRIS camera in detail.
[SIS]	The OSIRIS EDR/SIS document (detailed PDS label description)

3.5.6 The INDEX directory

The INDEX directory contains three index tables:

INDEX.TAB	The main index of all images in the dataset.
BROWSE_INDEX.TAB	The index of all the quicklook JPEG images included in the dataset.

3.5.7 The BROWSE directory

The BROWSE directory contains a copy of all the images stored in the DATA directory of the dataset stored in JPEG format. The structure is described in the BROWINFO.TXT file located in the root of the BROWSE data structure.

The images are stored using the same organization as used for the DATA directory with the images stored in <year>_<month> sub folders.

The images are stored in full resolution but downsampled from 16bit to 8 bit format using a histogram normalization method.

3.5.8 The EXTRAS directory

EXTRINFO.TXT	File describing the content of the EXTRAS directory .
AAREADME.HTM	Entry point into a HTML based browsing interface included in the dataset.
BROWSEHTML	Directory containing html file used by AAREADME.HTML
THUMBNAIL	Folder containing thumbnail versions of all the images stored in the DATA directory. The thumbnails are organized using <year>_< month> subfolders. The images have been downsampled to a size smaller than or equal to 128x128 and the images have been down scaled from 16+bit to 8bit using a histogram normalization method.
ACTIVITY.TAB	A time sorted overview index giving the relationship between operation activity/observation and acquired image.

3.6 Data File Naming Conventions and Product IDs

3.6.1 Filenaming Convention

The OSIRIS image files as archived in the PDS use the following filename convention:

CYYYYMMDDTHHMMSSUUUFFLIFAB.IMG

Field	Description
C	either N NAC (narrow angle camera) or W WAC (wide angle camera)
YYYY	is the year of acquisition
MM	is the month of acquisition
DD	is the day of acquisition
T	is the letter T (stands for "Time")
HH	is the hour of acquisition
MM	is the minute of acquisition
SS	is the second of acquisition
UUU	is the milli-second of acquisition
FF	is the image file type: the following filetypes are possible: ID Image Data (Normal images) TH Thumbnail version of the image (Highly compression version transmitted immediately) PA Amplifier A pre pixels (calibration data) PB Amplifier B pre pixels (calibration data) OL Overclocked lines (calibration data)
L	is the CODMAC processing level of the image
I	is the instance id if the image (multiple transmissions of an image will be reflected in this number incrementing)
F	is the letter F (stands for "Filter")
A	is the position index of the filter wheel #1
B	is the position index of the filter wheel #2
.IMG	File extension

Table 5 OSIRIS PDS data file filename elements

Example:

W20040923T071606570ID12F12.img

Is a WAC image acquired at 2004-09-23 at 07:16:06.657 UTC

The file contains CCD image data (image type ID) with raw image data (level 1) and the image represents the 2nd transmission of the image data. The image was acquired using the filter combination (1,2) = Hole+Red for the WAC.

The filename contains an approximate time of exposure. Please note that this time value is not very precise. The filename time value has not been corrected for spacecraft clock drift and leap seconds and will generally be around 18 s off. If a precise time vaoue is required please use the value store in the START_TIME field included in all header labels.

3.6.2 The Dataset ID

The OSIRIS DATA_SET_ID follows the following convention:

DATA_SET_ID = RO-<target id>-OSIRIS-<CODMAC level>-<mission phase abbreviation>-<description>-<version>

Field	Description
RO-	The letters "RO-"
<target ID>	A single letter code for the target type observed. (See Table 5 of RO-EST-TN-3372_1_ - for full list) A subset is: E = Earth M = Mars C = Comet A = Asteroid
-	The letter "-"
<Instrument>	Either OSINAC or OSIWAC
-	The letter "-"
<CODMAC level>	The CODMAC data level of the dataset (See Table 3)
-	The letter "-"
<mission phase ID>	One of the words: CVP, EAR1, CR2, MARS, CR3, EAR2, CR4A, AST1, CR4B, EAR3, CR5, AST2, RVM1, CR6, RVM2
-	The letter "-"
<mission phase name>	One of the words: COMMISSIONING, EARTHSWINGBY1, CRUISE2, MARSSWINGBY, CRUISE3, EARTHSWINGBY2, CRUISE4A, STEINSFLYBY, CRUISE4B, EARTHSWINGBY3, CRUISE5, LUTETIAFLYBY, RENDEZVOUSMANOEUVRE1, CRUISE6, RENDEZVOUSMANOEUVRE2



version	<p>The release version using the form: V<release>.<submission></p> <p>Example. V1.1 means release 1 submission 1</p> <p>The release number only increments if a dataset is resubmitted and made public. The submission number refers to deliveries of the same dataset from OSIRIS to the PSA (for example as part of the review process)</p>
---------	---

Example: RO-M-OSINAC-1-MARS-MARSSWINGBY-V1.0

3.7 Standards Used in Data Product Generation

3.7.1 PDS Standards

The OSIRIS archive is based on the PDS v3.6 specifications

3.7.2 Time Standards

3.7.2.1 SCLK Time fields

The SCLK time fields are specified using the following convention:

<reset number>/<time counter high value>:<time counter low value>

<time counter high value> is approximately the number of seconds since Jan 1 2003

<time counter low value> is counted in 1/65536 second ticks

Example:

1/37673377:42320

3.7.2.2 Calendar Time Fields

All time fields follow the ANSI time definition:

YYYY-MM-DDTHH:MM:SS.mmm

Where:

YYYY is the year in 4 digits

MM is the month in 2 digits

DD is the day of month in 2 digits

HH is the hour in 2 digits

MM is the minute in 2 digits

SS is the second in 2 digits

Mmm is millisecond

All time fields are given in UTC.

3.7.3 Reference Systems

The OSIRIS PDS labels uses references to a number of reference systems

3.7.3.1 Earth mean equator and equinox of J2000 (EME J2000)

International astronomical inertial reference frame (epoch J2000)

3.7.3.2 The Rosetta spacecraft coordinate frame:

The Rosetta spacecraft coordinate frame (S/C-COORDS) is defined with the +Z axis orthogonal to the instrument panel (average pointing of remote sensing instruments). The +Y axis is oriented along the solar panels and the +X is orthogonal to the high gain antenna mounting panel. The Rosetta spacecraft coordinate frame can be addressing in the SPICE system using the coordinate frame alias "ROS_SPACECRAFT".

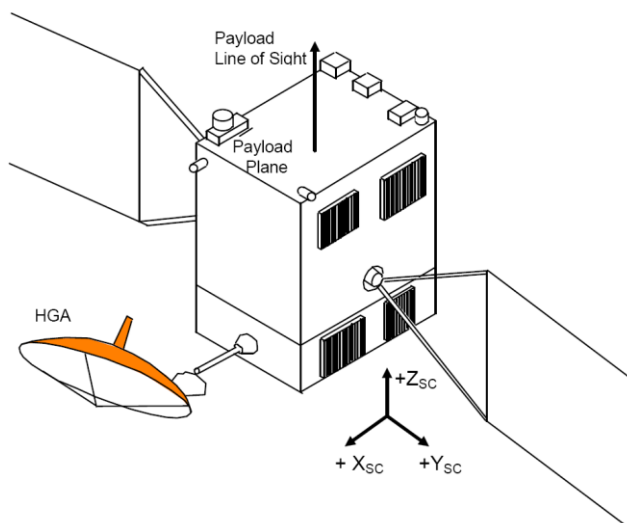


Figure 5 The Rosetta spacecraft coordinate frame (S/C-COORDS) definition

3.7.3.3 Camera Frames:

NAC CAMERA FRAME:

The NAC_CAMERA_FRAME is defined with origin at the center of the entrance aperture of the NAC camera with the +X axis along the image horizontal axis and the +Y axis along the vertical image direction. The +Z axis is defined as the right hand coordinate system defined by +X and +Y. Please note that for the NAC the +Z axis points in the opposite direction of the viewing direction.



The exact transformation can be found using the CAMERA_COORDINATE_SYSTEM label group in NAC images.

WAC CAMERA FRAME:

The WAC_CAMERA_FRAME is defined with origin at the center of the entrance aperture of the NAC camera with the +X axis along the image horizontal axis and the +Y axis along the vertical image direction. The +Z axis is defined as the right hand coordinate system defined by +X and +Y. Please note that for the WAC the +Z axis is pointed in the same direction as the boresight viewing direction.

The exact transformation can be found using the CAMERA_COORDINATE_SYSTEM label group in WAC images.

Please see the OSIRIS EDR/SIS for more detailed information

4 PDS Object and Keyword Definitions

The OSIRIS image data is stored as data files with embedded PDS label:

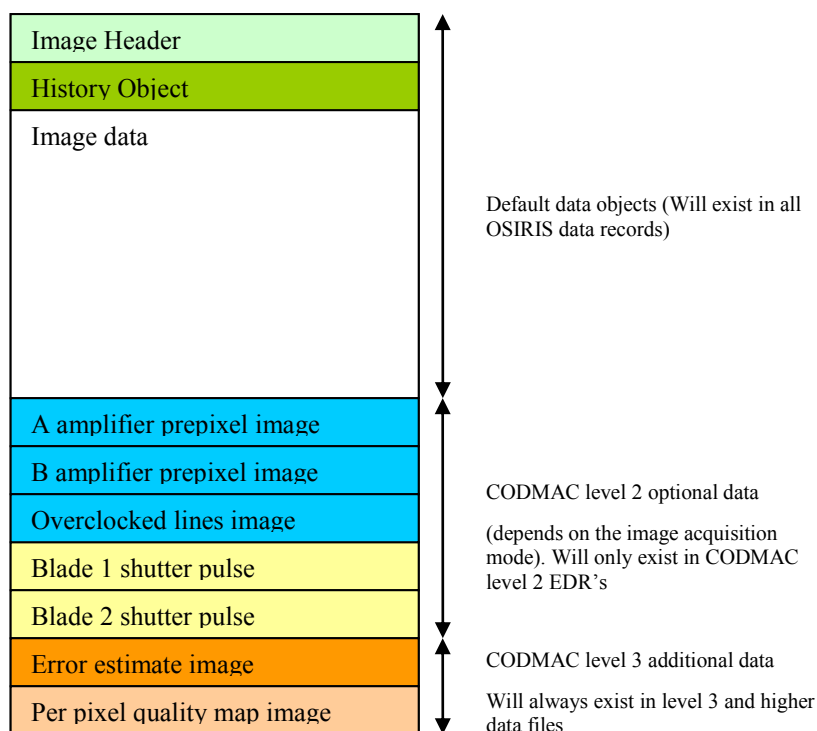


Figure 6 The OSIRIS data file organization

The used data formats are:

(EDR) 16bit unsigned integer data in low endian format (INTEL)

(RDR) 32bit PC_REAL data (INTEL single precision real)

The data is stored using a PDS IMAGE object for data definition:

IMAGE.LINES	gives the height of the image
IMAGE.LINE_SAMPLES	gives the width of the image
IMAGE.FIRST_LINE_SAMPLE	gives the horizontal image offset
IMAGE.FIRST_LINE	gives the vertical image offset

The binary offset of the start of the data can be determined using the PDS pointer label ^IMAGE.

Please see the OSIRIS EDR/SIS for more detailed information on the organization of the OSIRIS data files and the detailed definition of the OSIRIS PDS labels. The EDR/SIS can be found in the Document folder of the dataset in the SIS subfolder..